Radial buckling of multi-walled carbon nanotubes under hydrostatic pressure

Jin-Xing Shi · Toshiaki Natsuki · Qing-Qing Ni

Abstract Radial buckling stresses of carbon nanotubes (CNTs) need to be studied in high-pressure resonance Raman scattering spectrum. In this work, the closed-form expression of the critical buckling stress of multi-walled carbon nanotubes (MWCNTs) under hydrostatic pressure is derived that can be conveniently employed. Using the derived formulae, the critical buckling stresses of single-walled carbon nanotubes and double-walled carbon nanotubes with different diameters are calculated. The results are in good agreement with other reported literatures. In addition, the critical buckling stresses of each layer of a quintuple-walled CNT in different buckling modes are predicted, showing that the buckling instability can occur not only in the outermost rolled layer, but also in other rolled layer of MWCNTs by considering different diameters and buckling modes.

1 Introduction

The physics of carbon nanotubes (CNTs) has rapidly evolved into a research field soon after the landmark literatures reported by Iijima on multi-walled carbon nanotubes (MWCNTs) in 1991 [1] and single-walled carbon nanotubes (SWCNTs) 2 years later [2]. Since then, theoretical and experimental studies in different fields have focused on both the fundamental physical properties and the potential applications of CNTs [3]. Raman spectroscopy (RS) is a valuable tool to study CNTs under high pressure for the investigation of application on their mechanical and structural stability [4]. Resonance RS allows the selective probing of different CNTs, and several hydrostatic pressure Raman investigations on CNTs were carried out [5–8]. Venkateswaran et al. [5] reported the effects of hydrostatic pressure on the first-order Raman scattering spectrum of SWCNT bundles excited with 2.41 eV. They found that the radial mode intensity disappears beyond 1.5 GPa, and the tangential mode intensity also drops considerably above the pressure. Therefore, in high-pressure resonance Raman scattering, the radial buckling instability of CNTs needs to be investigated.

Investigations of buckling instability property of CNTs have focused on both experimental [9–15] and theoretical methods [16–24]. Tang et al. [9] reported a measurement of mechanical deformation of SWCNTs under hydrostatic high pressure using a diamond anvil cell and in situ X-ray diffraction, and obtained that SWCNTs show linear elasticity under hydrostatic pressure up to 1.5 GPa at room temperature. Within a transmission electron microscope, Tsai et al. [15] investigated buckling deformation of an individual MWCNT through in situ nanoindentation. The in situ observations revealed a significant shell-to-Euler phase transformation in the buckling response of the nanotube. However, it is still difficult to perform experiment on testing individual CNTs, especially for the radial compression buckling under hydrostatic pressure. Thus, theoretical methods, such as molecular dynamics (MD) simulation and continuum mechanics, have been widely

J.-X. Shi
Interdisciplinary Graduate School of Science and Technology, Shinshu University, 3-15-1 Tokida, Ueda-shi, Nagano 386-8567, Japan

T. Natsuki (✉) · Q.-Q. Ni
Faculty of Textile Science and Technology, Shinshu University, 3-15-1 Tokida, Ueda-shi, Nagano 386-8567, Japan
e-mail: natsuki@shinshu-u.ac.jp

T. Natsuki
Institute of Carbon Science and Technology, Shinshu University, 4-17-1 Wakasato, Nagano-shi, Nagano 380-8553, Japan

utilized in studying the mechanical properties of CNTs. Based on MD simulation, Wang et al. [16] studied the local buckling instability of a SWCNT subjected to point loading, in which a mechanical model is developed and verified to predict the onset of the local instability.

On the other hand, although CNTs can have diameters only several times larger than the length of a bond between carbon atoms, continuum models have been found to describe their mechanical behavior very well under many circumstances [24]. Ansari et al. [25] developed a nonlocal Flügge shell model incorporating interatomic potentials to study the buckling instability of an axially loaded SWCNT. The proposed model is independent of the widely scattered values of Young's modulus and effective thickness of nanotubes, which is a distinguishing feature. Hydrostatic pressure can yield a distinct class of buckling, reflecting the high flexibility of graphene sheets in the normal direction in the radial compression buckling instability of CNTs [26]. Natsuki et al. [18] presented a continuum shell model to study the elastic buckling of SWCNTs and DWCNTs subject to hydrostatic pressure. Based on this model, the critical buckling stress of a SWCNT with a diameter of 1.3 nm is calculated about 1.6 GPa by a nontrivial solution.

The present work aims to derive the formulae of the critical buckling stress of MWCNTs under hydrostatic pressure that can be used conveniently for predicting the radial buckling stress of MWCNTs. In Sect. 2, based on an elastic continuum model, the formulae of the critical buckling stress of MWCNTs under hydrostatic pressure are derived from a mathematic method. In Sect. 3, using the derived formulae, the radial buckling stresses of SWCNTs and MWCNTs under hydrostatic pressure are calculated. The influences of diameter of CNTs, buckling mode and the layer number of MWCNTs to the critical buckling stresses are discussed in detail. Moreover, for a given example of quintuple-walled CNTs, on which layer the critical buckling can occur is also discussed in detail by considering different diameters and buckling modes. At last, conclusions are shown in Sect. 4.

2 Theoretical approach

CNTs are usually modeled by cylindrical shells [24]. In analyzing the buckling of cylindrical shells under hydrostatic pressure, the circumferential compressive stress is of great importance. For CNTs with large aspect ratio, the critical value of the external pressure only slightly affects the boundary conditions prescribed on the shell edges of CNTs. This means that a distortion of the circular cross section will be identical throughout the length of the shell. Hence, the buckling analysis of CNTs with large aspect ratio can be replaced by analyzing the stability of a ring of

unit length with the same radius and thickness. The critical buckling value of the circumferential compressive pressure P_{cr} is given by [27]

$$P_{cr} = \frac{(n^2 - 1)EI}{r^3} \tag{1}$$

where n is the number of half-waves in the circumferential direction, E and I are Young' modulus and the moment of inertial, and r is the radius of the ring.

Figure 1a shows an analytical model of the cross section of a MWCNT with N rolled layers under hydrostatic pressure p_{hy}. r_i $(i = 1, N)$ is the radius of the ith rolled layer of MWCNTs. Then, the circumferential compressive force P_i $(i = 1, N)$ on each rolled layer of the MWCNT can be written as

$$P_1 = p_{12}$$
$$\vdots$$
$$P_i = p_{i(i-1)} + p_{i(i+1)} \quad (i = 2, \ldots, N - 1) \tag{2}$$
$$\vdots$$
$$P_N = p_{N(N-1)} + p_{hy}$$

where $p_{ij} = -p_{ji} = c_{ij}(\Delta w_i - \Delta w_j)$ $(i, j = 1, N)$ are the vdW interaction forces on the ith rolled layer shown in Fig. 1b, where Δw_i $(i = 1, N)$ is the transverse deflection of the ith rolled layer, and c_{ij} is the vdW interaction coefficient between the ith and the jth rolled layer that can be estimated from the Lennard-Jones potential, given as [28]

$$c_{ij} = \frac{\pi \varepsilon r_j \sigma^6}{3a^4} \left(1001 \sigma^6 H_{ij}^{13} - \frac{1120}{3} H_{ij}^7 \right) \tag{3}$$

where

$$H_{ij}^m = (r_i + r_j)^{-m} \int_0^{\frac{\pi}{2}} \frac{d\theta}{\left(1 - K_{ij} \cos^2 \theta \right)^{\frac{m}{2}}} \quad (m = 7, 13) \tag{4}$$

and

$$K_{ij} = \frac{4 r_i r_j}{(r_i + r_j)^2} \tag{5}$$

where $a = 0.142$ nm is the carbon–carbon bond length, and σ and ε are the vdW radius and the well depth of the Lennard-Jones potential, respectively. The vdW parameters in the Lennard-Jones potential are $\sigma = 0.34$ nm and $\varepsilon = 2.967$ meV as reported by Saito et al. [29].

The deflection Δw corresponds to a hoop stress produced from internal pressure P. In the present work, Δw is considered to be the inward deflection of nanotube wall prior to buckling. Thus, the corresponding net transverse pressure P prior to buckling is expressed as [30, 31]

Fig. 1 Schematic model of MWCNTs. **a** Cross section of a MWCNT consisted of N rolled layers under hydrostatic pressure p_{hy} and **b** the vdW interaction forces on the ith rolled layer

(a)

(b)
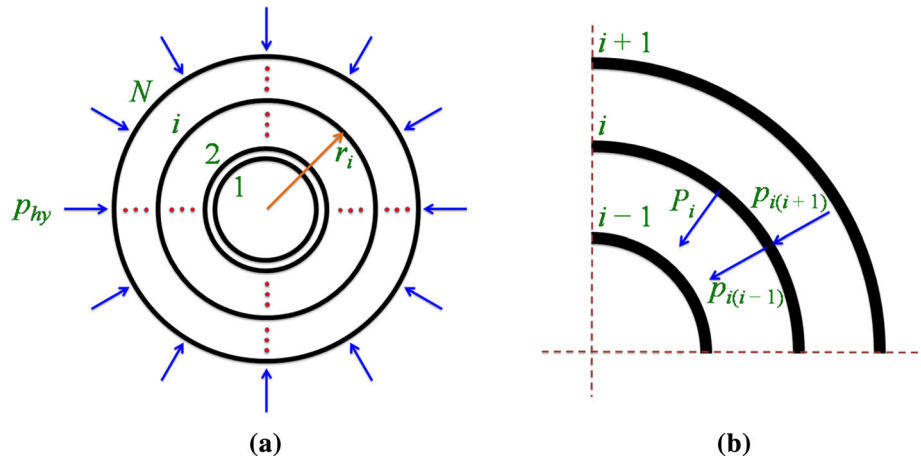
$$P = -Et\frac{\Delta w}{r^2} \tag{6}$$

where t is the thickness of rolled layer.

Considering the vdW interaction coefficient given in Eq. (3), substitution of Eq. (6) into Eq. (2) yields

$$P_1 = p_{12} = c_{12}(\Delta w_1 - \Delta w_2) = -Et\frac{\Delta w_1}{r_1^2}$$

$$\vdots$$

$$P_i = p_{i(i-1)} + p_{i(i+1)} = c_{i(i-1)}(\Delta w_i - \Delta w_{(i+1)})$$
$$+ c_{i(i+1)}(\Delta w_i - \Delta w_{(i+1)}) = -Et\frac{\Delta w_i}{r_i^2} \quad (i = 2,\ldots,N-1)$$

$$\vdots$$

$$P_N = p_{N(N-1)} + p_{hy} = c_{N(N-1)}(\Delta w_N - \Delta w_{N-1})$$
$$+ p_{hy} = -Et\frac{\Delta w_N}{r_N^2} \tag{7}$$

Eq. (7) can be rewritten as
where

$$X_1 = \frac{c_{12}r_1^2}{c_{12}r_1^2 + Et}$$

$$\vdots$$

$$X_i = \frac{c_{i(i+1)}r_i^2}{\left(c_{i(i-1)} + c_{i(i+1)} - c_{i(i-1)}X_{i-1}\right)r_i^2 + Et}$$
$$(i = 2,\cdots,N-1) \tag{9}$$

$$\vdots$$

$$X_N = \frac{c_{N(N-1)}r_N^2}{c_{N(N-1)}r_N^2 + Et}$$

and

$$\alpha = \frac{r_N^2}{c_{N(N-1)}r_N^2 + Et} = \frac{X_N}{c_{N(N-1)}} \tag{10}$$

Here, a mathematic method is proposed to derive the formulae of the critical buckling of MWCNTs under circumferential compressive pressure. From Eq. (8), we obtain

$$\begin{pmatrix} 1 & -X_1 & & & & \\ & 1 & -X_2 & & & \\ & & \vdots & & & \\ & & & -X_i & & \\ & & & \vdots & & \\ & & & & 1 & -X_{N-1} \\ & & & & -X_N & 1 \end{pmatrix} \begin{Bmatrix} \Delta w_1 \\ \Delta w_2 \\ \vdots \\ \Delta w_i \\ \vdots \\ \Delta w_{N-1} \\ \Delta w_N \end{Bmatrix} = \begin{Bmatrix} 0 \\ 0 \\ \vdots \\ 0 \\ \vdots \\ 0 \\ -\alpha p_{hy} \end{Bmatrix} \quad (i = 3,\cdots,N-2) \tag{8}$$

$$\Delta w_N = \frac{-\alpha p_{hy}}{1 - X_{N-1}X_N}$$

$$\Delta w_{N-1} = \frac{-\alpha X_{N-1}p_{hy}}{1 - X_{N-1}X_N} = X_{N-1}\Delta w_N$$

$$\vdots$$

$$\Delta w_i = X_i \Delta w_{i+1} \quad (i = 3, \cdots, N-2) \tag{11}$$

$$\vdots$$

$$\Delta w_2 = X_2 \Delta w_3$$

and

$$\Delta w_1 = X_1 \Delta w_2 = \Delta w_N \prod_{k=1}^{N-1} X_k = \frac{-\alpha p_{hy}}{1 - X_{N-1}X_N} \prod_{k=1}^{N-1} X_k \tag{12}$$

Substituting Eq. (12) into Eq. (11), all of Δw_i ($i = 1$, N) can be expressed by X_i ($i = 1$, N) shown in Eq. (9). Then, from a link between the internal pressure P and the critical buckling pressure P_{cr} by substituting these Δw_i ($i = 1$, N) into Eq. (1) and using Eq. (7), the formulae of the critical buckling stress of each rolled layer of MWCNTs under hydrostatic pressure can be finally derived and shown as

$$p_{cr,N} = \frac{(n^2 - 1)I}{r_N \alpha t}(1 - X_{N-1}X_N)$$

$$\vdots$$

$$p_{cr,i} = \frac{(n^2 - 1)I}{r_i \alpha t}(1 - X_{N-1}X_N) \prod_{k=i}^{N-1} \frac{1}{X_k} \quad (i = 1, \cdots, N-1) \tag{13}$$

3 Analytical results and discussion

According to the theoretical approach, the formulae of the critical buckling stress of MWCNTs were carried out based on the cylindrical shell model. In this research, to study the buckling properties of MWCNTs under hydrostatic pressure, each rolled layer is modeled as an individual cylindrical shell of unit length. The effective thickness of each layer of MWCNTs is 0.066 nm. The space between nanotube walls is 0.34 nm. CNTs have the effective stiffness of $Et = 360$ J/m and Poisson's ratio of 0.27 [18].

The minimum value of critical buckling stress is usually reached when $n = 2$. Using Eq. (13), the relationship between the critical buckling stress and diameter of SWCNTs in buckling mode $n = 2$ is shown in Fig. 2. As the diameter of SWCNTs increases, the critical buckling press decreases nonlinearly. The reason is that with the increasing diameter, the elastic modulus of SWCNTs decreases rapidly. Thus, the critical buckling stress is highly sensitive to small-diameter SWCNTs and decreases with an increase of the diameter. Furthermore, a comparison of the critical buckling stresses on SWCNTs under
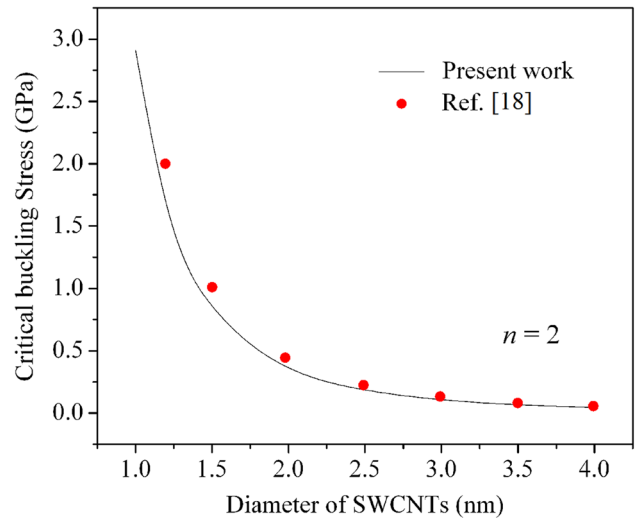

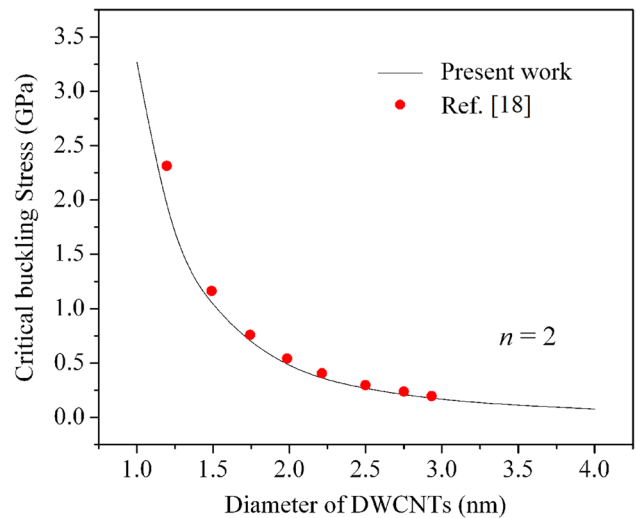**Fig. 2** Relationship between the critical buckling stress and diameter of SWCNTs

Fig. 3 Relationship between the critical buckling stress and diameter of DWCNTs

hydrostatic pressure is also shown in Fig. 2. The critical buckling stresses for buckling mode $n = 2$ based on Eq. (13) are in good agreement with those obtained from Ref. [18]. For example, the critical buckling stress of SWCNT with a diameter 1.3 nm is calculated as 1.32 GPa in the present work, which is in agreement with about 1.6 GPa reported in Ref. [18] and 1.5 GPa reported in Ref. [5].

For MWCNTs, the vdW interaction forces between the nanotubes are considered in Eq. (7). To judge the robustness of the proposed formulae for MWCNTs containing vdW interaction forces, a comparison of the critical radial buckling stress of DWCNTs in buckling mode $n = 2$
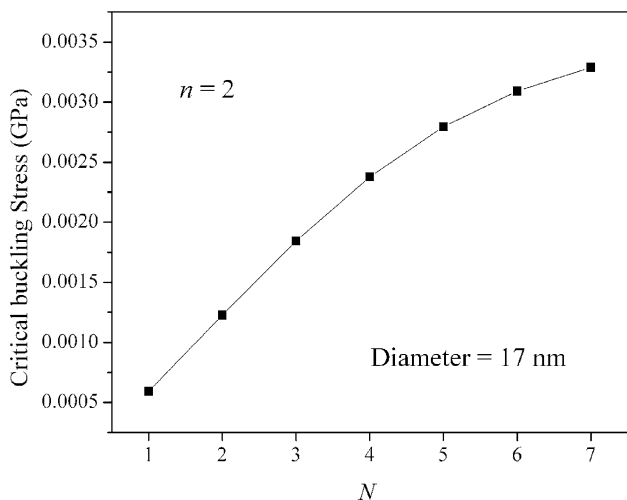
Fig. 4 Variation of the critical buckling stress on the outermost nanotube of MWCNTs with different rolled layers N

Fig. 5 The critical buckling stress in different buckling modes on the ith rolled layer of quintuple-walled CNTs

derived from Eq. (13) and Ref. [18] is shown in Fig. 3. They are also in a good agreement with each other. The critical buckling stress decreases with increasing diameter of DWCNTs, which is the same as SWCNTs shown in Fig. 2. Comparing with Figs. 2 and 3, DWCNTs can endure higher critical radial buckling stress than SWCNTs in the same diameter. The reason is that the stiffness of DWCNTs can be enhanced by the inner nanotube through the vdW interaction forces.

In the case of MWCNTs with rolled layer number $N \geq 3$, based on Eq. (13), critical radial buckling stress of the outermost nanotube of MWCNTs with the same diameter 17 nm in buckling mode $n = 2$ is shown in Fig. 4 as a function of rolled layer number N. The results show that a MWCNT with larger rolled layer number has higher buckling stability, because of the enhancement of the inner nanotubes through the vdW interaction forces. If N varies from 1 to 5, the critical buckling stress on CNTs increases from 0.59 to 3.3 MPa, so that it is increased by 5.6 times.

In actual, because different buckling modes can occur in each rolled layer of MWCNTs, the buckling instability can happen in different rolled layers in MWCNTs by considering the diameter of MWCNTs. For this reason, a quintuple-walled CNT consisting of five rolled layers with a diameter of 17 nm is chosen to discuss this issue. Figure 5 shows the critical buckling stress in different buckling modes on each nanotube of a quintuple-walled CNT. Buckling stresses of each layer increase as buckling mode increases. For instance, the critical radial buckling stress on the third layer of a quintuple-walled CNT increases from 7.5 to 15.3 MPa when buckling mode n is from 2 to 4.
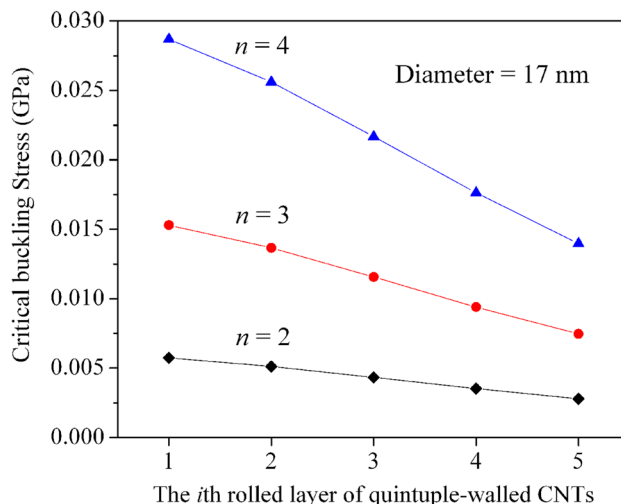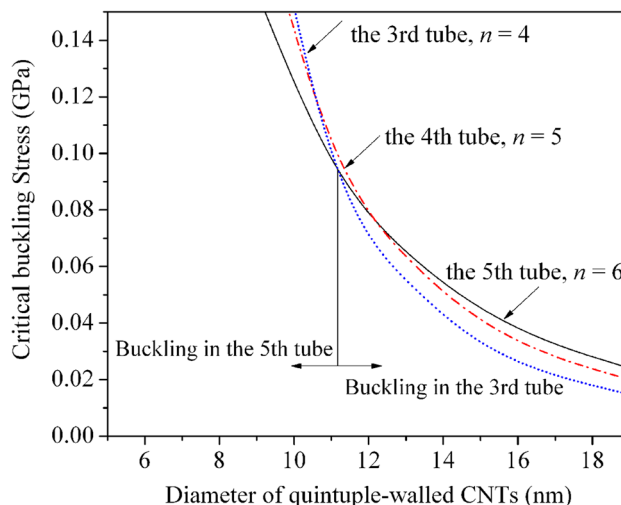

Fig. 6 The critical buckling stress of quintuple-walled CNTs as a function of diameter of MWCNTs

However, as shown in Fig. 5, the critical buckling stress of the fifth wall in mode $n = 3$ is higher than the critical buckling stresses of the first, second, third and fourth walls in mode $n = 2$. In this case, the buckling instability can happen on one of the inner walls (the first, second, third and fourth walls) in buckling mode $n = 2$, instead of on the outmost wall (the fifth wall) in higher mode ($n = 3$). To illustrate this issue in detail, the critical buckling stress of a quintuple-walled CNT as a function of nanotube diameter is shown in Fig. 6 as an example. The dotted, dashed and solid lines represent the buckling stresses of the third, fourth and fifth nanotubes in buckling mode $n = 4$, $n = 5$ and $n = 6$, respectively. It is clearly seen that all of the

three lines decrease significantly with an increase in the diameter of the quintuple-walled CNT. Furthermore, the dashed line and the solid line intersect in a key point, which is (11.14 nm, 0.095 GPa). Before the key point, the solid line is the lowest curve, whereas the dotted line is the lowest curve when the diameter of quintuple-walled CNTs is larger than 11.14 nm. Thus, in the given example, the buckling instability should occur on the fifth nanotube in $n = 6$ when the diameter of quintuple-walled CNTs is smaller than 11.14 nm and occur on the third nanotube in $n = 4$ when the diameter is larger than the key point.

4 Conclusions

In this work, the buckling analysis on MWCNTs considering the vdW interaction forces between the nanotubes was carried out based on a theoretical approach. We derived the closed-form expression that can directly apply on calculating the critical buckling stress on MWCNT. Using the buckling formulae of CNTs, we calculated the critical buckling stresses of SWCNTs, DWCNTs and quintuple-walled CNTs under hydrostatic pressure. The results obtained from SWCNTs and DWCNTs are in good agreement with other published results, which can judge the robustness of the proposed formulae. The critical buckling stress decreases significantly as the diameter of CNTs increases, especially in the case of small diameters. The critical buckling stress of each layer of MWCNTs is significantly affected by buckling mode and increases as buckling mode increases. Moreover, an example to analyze the critical buckling stresses of the third, fourth and fifth walls of a quintuple-walled CNT in different buckling mode $n = 4$, $n = 5$ and $n = 6$ was given. The results showed that the buckling instability on MWCNTs can occur not only in the outermost rolled layer, but also in other rolled layer of MWCNTs according to diameter and buckling mode.

References

1. S. Iijima, Nature **354**, 56 (1991)
2. S. Iijima, T. Ichihashi, Nature **363**, 603 (1993)
3. S. Reich, C. Thomsen, J. Maultzsch, *Carbon nanotubes: basic concepts and physical properties* (WILEY-VCH Verlag GmbH & Co. KGaA, Weinheim, 2004)
4. I. Loa, J. Raman Spectrosc. **34**, 611 (2003)
5. U.D. Venkateswaran, A.M. Rao, E. Richter, M. Menon, A. Rinzler, R.E. Smalley, P.C. Ecklund, Phys. Rev. B **59**(10), 928 (1999)
6. P. Puech, A. Ghandour, A. Sapelkin, C. Tinguely, E. Flahaut, D.J. Dunstan, W. Basca, Phys. Rev. B **78**, 045413 (2008)
7. L. Alvarez, J.L. Bantignies, R. Le Parc, R. Aznar, J.L. Sauvajol, A. Merlen, D. Machon, A. San Miguel, Phys. Rev. B **82**, 205403 (2010)
8. A.L. Aguiar, A. San-Miguel, E.B. Barros, M. Kalbáč, D. Machon, Y.A. Kim, H. Muramatsu, M. Endo, A.G. Souza Filho, Phys. Rev. B **86**, 195410 (2012)
9. J. Tang, L.C. Qin, T. Sasaki, M. Yudasaka, A. Matsushita, S. Iijima, Phys. Rev. Lett. **85**, 1887 (2000)
10. J.F. Waters, L. Riester, M. Jouzi, P.R. Guduru, J.M. Xu, Appl. Phys. Lett. **85**, 1787 (2004)
11. Y.R. Jeng, P.C. Tsai, T.H. Fang, Appl. Phys. Lett. **90**, 161913 (2007)
12. H.W. Yap, R.S. Lakes, R.W. Carpick, Nano Lett. **7**, 1149 (2007)
13. P.R. Guduru, Z. Xia, Exp. Mech. **47**, 153 (2007)
14. D.Y. Khang, J. Xiao, C. Kocabas, S. MacLaren, T. Banks, H. Jiang, Y.Y. Huang, J.A. Rogers, Nano Lett. **8**, 124 (2008)
15. P.C. Tsai, Y.R. Jeng, Y.X. Huang, K.T. Wu, Appl. Phys. Lett. **103**, 053119 (2013)
16. Q. Wang, K.M. Liew, X.Q. He, Y. Xiang, Appl. Phys. Lett. **91**, 093128 (2007)
17. Q. Wang, K.M. Liew, V.K. Varadan, Appl. Phys. Lett. **92**, 043120 (2008)
18. T. Natsuki, N. Fujita, Q.Q. Ni, M. Endo, J. Appl. Phys. **106**, 084310 (2009)
19. J.X. Shi, T. Natsuki, X.W. Lei, Q.Q. Ni, ASME J. Nanotechnol. Eng. Med. **3**, 020903 (2012)
20. S.C. Pradhan, G.K. Reddy, Comp. Mater. Sci. **50**, 1052 (2011)
21. X. Huang, W. Liang, S. Zhang, Nanoscale Res. Lett. **6**, 53 (2011)
22. B. Motevalli, A. Montazeri, J.Z. Liu, H. Rafii-Tabar, Comp. Mater. Sci. **79**, 619 (2013)
23. D.D.T.K. Kulathunga, K.K. Ang, Comp. Mater. Sci. **81**, 233 (2014)
24. D. Qian, G.J. Wagner, W.K. Liu, M.F. Yu, R.S. Ruoff, Appl. Mech. Rev. **55**, 495 (2002)
25. R. Ansari, R. Gholami, S. Sahmani, Appl. Phys. A **113**, 145 (2013)
26. H. Shima, Materials **5**, 47 (2012)
27. E. Ventsel, T. Krauthammer, *Thin plates and shells* (Marcel Dekker Inc, New York, 2001)
28. X.Q. He, S. Kitipornchai, K.M. Liew, J. Mech. Phys. Solids **53**, 303 (2005)
29. R. Saito, R. Matsuo, T. Kimura, G. Dresselhaus, M.S. Dresselhaus, Chem. Phys. Lett. **348**, 187 (2001)
30. S. Timoshenko, S. Woinowsky-Keieger, *Theory of plates and shells* (McGraw-Hill Book Co., Singapore, 1959)
31. X. Wang, G. Lu, Y.J. Lu, Int. J. Solids Struct. **44**, 336 (2007)